Total photoionization cross sections of atomic oxygen from threshold to 44.3Å

G.C. Angel and James A.R. Samson

Behlen Laboratory of Physics

University of Nebraska

Lincoln, NE 68588-0111

ABSTRACT

The relative photoionization cross section of atomic oxygen for the production of singly charged ions has been remeasured in more detail and extended to cover the wavelength range 44.3 to 910.5Å by use of synchrotron radiation. In addition, the contribution of multiple ionization to the cross sections has been measured allowing total photoionization cross sections to be obtained below 250Å. The results have been made absolute by normalization to our previously measured data. The use of synchrotron radiation has enabled measurements of the continuum cross section to be made between the numerous autoionizing resonances that occur near the ionization thresholds. This in turn has allowed a more critical comparison of the various theoretical estimates of the cross section to be made. The series of autoionizing resonances leading to the ^4P state of the oxygen ion have been observed for the first time in an ionization type experiment and their positions have been compared with both theory and previous photographic recordings.

I. INTRODUCTION

It has long been realized that the photoionization of atomic oxygen plays an important role in the interpretation of solar-terrestrial effects and in the study of stellar atmospheres. Experimental difficulties associated with its measurement, however, meant that, for many years, a knowledge of the magnitude of the photoionization cross section was limited to theoretical estimates. The first calculation was made by Bates et al.[1] in 1939 using a Hartree-Fock approximation, but it was not until 1949 that Bates and Seaton[2] reported more detailed calculations that took into account the effect of exchange. Since then many authors[3-16] have reported calculations that incorporate increasing degrees of sophistication and complexity associated with the photon-atom interaction. An interesting review on the progress of our understanding of the photoionization of atomic oxygen since 1939 has been given recently by Seaton.[17]

The first absolute measurement of the atomic oxygen photoionization cross section was made in 1965 by Cairns and Samson [18] who used an absorption tube technique to measure its total absorption cross section. It was remeasured by Comes et al.[19] using a crossed beam method, but the agreement was not good. Subsequent measurements by Kohl et al.[20] were made covering a limited energy range using the dissociation produced in a shock heated gas. In 1985 Samson and Pareek[21] reported absolute measurements made using a mass spectrometric technique; they also showed that for photon energies above ~ 25eV the atomic cross section was very close to one-half of the total molecular ionization cross section. Huffman et al.[22] used a photographic technique to classify the autoionizing resonances leading to the $^4S^\circ$, $^2D^\circ$, and $^2P^\circ$ thresholds and Dehmer et al.[23] measured relative photoionization cross sections in the same region. In addition, several measurements have been made of the branching ratios for the production of

the $^4S^\circ$, $^2D^\circ$, and $^2P^\circ$ states,[24-26] and of the angular distributions of the ejected photoelectrons.[25,27]

The purpose of the present experiment was to remeasure the relative photoionization cross section of atomic oxygen, including the effects of multiple ionization, over as wide an energy range as possible using the continuum radiation available from a synchrotron storage ring. This would also allow more detailed measurements at the ionization threshold to be made. In addition, a clearer picture of the variation of the continuum cross section between the autoionizing resonances from the $^4S^\circ$ to the $^2P^\circ$ ionization thresholds could be obtained, in order to give an indication which of the presently available theories describes most closely the ionization process in this region. The continuum radiation would also allow observation of the Rydberg series $2s2p^4\ (^4P)np$, the presence of which had been indicated at only a few discrete wavelengths in our previous work.[21]

II. EXPERIMENTAL APPROACH AND ANALYSIS OF RESULTS

The experiment was performed at the University of Wisconsin synchrotron storage ring, Aladdin, using radiation from both a 4 meter normal incidence and a Mark II Grasshopper grazing incidence monochromator. Figure 1 shows a schematic diagram of the apparatus used in the experiment. Molecular oxygen was partially dissociated in a microwave discharge sustained by the air cooled cavity, C. The discharge, operated at 2450 MHz and with up to 100 watts microwave power, was initiated by a spark from a Tesla coil. The discharge products flowed along the pyrex tube, T, which was coated with phosphorus pentoxide to minimize recombination on the walls, and passed, via a 0.5mm orifice through the center of the collision region, R, and then to the turbo-molecular pump, P_1. The differential pumping region, D, evacuated by the turbomolecular pump, P_2, separated the relatively high pres-

sure collision region ($\sim 10^{-6}$ torr) from the ultra-high vacuum of the monochromator output mirror box ($\sim 5 \times 10^{-10}$ torr). Radiation passed via the low conductance canals, C_1 and C_2, through the middle of the collision region, R, and was then incident on the photon detector, M. This was either a sodium salicylate/photomultiplier combination or an aluminum photodiode, the current from either of which was recorded by a picoammeter. Ions produced in the collision region were extracted and focussed by the electrostatic lens system, L, onto the entrance of the 180° electromagnetic mass spectrometer, S, where the ions of interest were separated and directed to the first dynode of the Johnston type MM1 particle multiplier, J, the signal from which was recorded using particle counting techniques. The signals from the photon detector and the ion rate meter were simultaneously recorded on a strip chart recorder.

The experimental investigation was conducted as follows. Previous investigations in our laboratory have shown that the dissociation fraction produced by the microwave discharge requires a considerable period in which to stabalize but that once it has done so the atomic production remains essentially constant. Consequently, pure O_2 was admitted to the discharge tube via a needle valve and the microwave discharge struck. This was then left to stabalize for up to 4 hours. The electromagnet was tuned to select O^+ ions and the monochromator scanned over the wavelength range of interest. A similar scan was made of the parent molecular ion, the whole process being repeated with the microwave discharge extinguished. Repeat measurements were made at several discharge gas pressures between 200 and 700 microns and, in the case of the 4 meter monochromator, with both the photomultiplier and photodiode as photon detector.

The number, N^+, of ions produced when a flux I_o of photons passes through a gas whose number density/path length product is $n\ell$ is given by the equation

$$N^+ = I_o n\ell\sigma, \tag{1}$$

provided $n\ell\sigma \ll 1$, where σ is the photoionization cross section. If the ion extraction, analysis, and detection system has an overall efficiency F and if the efficiency of the photon detector is G then Eq. (1) becomes

$$N_D^+/F = (I_D/G)n\ell\sigma, \tag{2}$$

where N_D^+ and I_D are the ion count rates and photon signals, respectively, actually recorded. It may be seen that for constant n, ℓ, and F we obtain the expression

$$\sigma \propto (N_D^+/I_D)G. \tag{3}$$

Relative values for the efficiency G of the photodiode used in the experiment could be obtained by running a noble gas (neon or argon) through the collision region in place of the oxygen and recording the ion count rate and photo-diode signal simultaneously. Since the noble gas absorption cross sections σ(Ar, Ne) are known[28,29] Eq. (3) shows that

$$G \propto (I_D/N_D^+)\ \sigma\ (Ar, Ne). \tag{4}$$

For the salicylate screen/photomultiplier combination the efficiency is known to be constant up to photon energies of ~60eV;[30] this detector was never used for wavelengths shorter than ~400Å. Thus, using either photon detector, Eq. (3) may be used to determine the relative variation of the photoionization cross section for the gases under study.

Data were recorded on the 4 meter monochromator from well before the ionization threshold to approximately 400Å. Between the atomic ionization threshold (910.4Å) and 662Å the ion signal arose purely from the ionization of the atom; at wavelengths shorter than this a component caused by dissociative ionization was also present. At these wavelengths the relative atomic ionization cross section is given by the expression

$$\sigma \propto G[(N_D^+/I_D) - \alpha(N_D^+/I_D)_{off}], \tag{5}$$

where the second bracket represents the ion to photon ratio with the microwave discharge turned off and α is the fraction of molecular oxygen left undissociated. It should be noted, however, as observed by Samson and Pareek[21], that Eq. (5) is strictly true only in the absence of excited states of the oxygen molecule. Several groups[18,24,33] have shown that the production of atomic oxygen in a microwave discharge leads to the formation of molecular oxygen in its $a(^1\Delta)$ excited state. Thus, the presence of this species must be considered. However, it can be shown[21] that this has a negligible effect on the atomic cross section provided that the continuum photoionization cross section of O_2 in its ground $X(^2\Sigma_u)$ states is comparable to O_2 in the $a(^1\Delta)$ states. From the theoretical calculations of Roche et al.[34] it appears that this is a reasonable assumption.

The fraction α was determined from the molecular ion to photon ratio obtained from runs with the microwave generator turned on and off. It was found to be of the order 0.83 - 0.93 depending on the pressure in the discharge tube and the condition of the phosphorous pentoxide coating. Values for the ion count rate and photon signal were measured from the chart recorder traces at appropriate wavelengths, chosen to be at positions not influenced by the many autoionizing resonances observed. The relative cross sections were determined using either Eq. (3) or (5) depending on

whether the wavelength was above or below the dissociative ionization threshold. A further correction to the O^+ production cross section was necessary between 700 and 725Å because of the production of O^+ from the pair production reaction

$$h\nu + O_2 \rightarrow O^+ + O^-,$$

which was previously reported by Dehmer and Chupka[31] and which was clearly visible in the O^+ signal trace recorded with the microwave switched off. No new information could be gained from the width of the autoionizing resonances over that already obtained by Dehmer et al.[23] because the 4m monochromator, although having a designed resolution of .07A for a 100 micron exit aperture, was found to have an actual resolution of 0.6A that was largely independent of the monochromator slit width. For this reason, and because of the number of peaks involved, values for the photoionization cross section have not been calculated over the autoionizing peaks.

Data on the grazing incidence monochromator were recorded from its long wavelength limit of 310Å to 44.3Å at which point considerable photon loss was apparent because of increasing absorption at the carbon K edge caused by carbon deposited on the mirrors and grating. All the oxygen ion signals, except O^{3+}, taken on this monochromator had dissociative ionization components associated with them. Thus Eq. (5) was used exclusively to determine the relative photoionization cross section. Equation (5) also applies in determining multiple ionization cross sections provided N_D^{n+} is substituted for N_D^+, where n is the degree of ionization. The relative cross section can then be placed on an absolute basis by determining the constant of proportionality for Eq. (5). This constant is the same for single or multiple ionization. More details on the multiple ionization of atomic oxygen are given in a separate paper.[35]

A major difficulty associated with the use of a continuum as opposed to a discrete line source is the separation of true signal from that arising from second and higher order spectra and scattered radiation. Subsidiary experiments were carried out on both monochromators to try to determine the extent of the contamination by unwanted radiation. On the 4 meter normal incidence monochromator using the photomultiplier detector the following technique was used.

At any particular wavelength it was assumed that the radiation consisted of components of both the first and second orders I_o' and I_o''. These in turn would produce ion signals N' and N'' with cross sections σ' and σ'', according to Eq. (2). In the experiment the measured ratio of ions per photon was given by

$$\text{Ratio} = \frac{(N_D' + N_D'')}{(I_D' + I_D'')} .$$

Thus,

$$\text{Ratio} = \frac{F/G(I_D' n\ell\, \sigma' + I_D'' n\ell \sigma'')}{(I_D' + I_D'')} .$$

Because F, G, L, and the number density/path length product $n\ell$ are assumed to be constant this may be reduced to

$$\text{Ratio} = \frac{C\,[\sigma' + (I_D''/I_D')\,\sigma'')]}{[1 + (I_D''/I_D')]} ,$$

where C is a constant. The ratio above could be determined at wavelengths just above and below the onset of ionization for a particular gas target yielding two equations for the two unknowns C and (I_D''/I_D'), where it is assumed that this ratio is constant over a restricted wavelength range. This process was carried out at the argon and neon ionization thresholds, (787Å and 575Å, respectively) and at the threshold for O_2^+ production (1026Å). (I_D''/I_D') was found never to exceed 4%. Higher order corrections to data gathered on the 4 meter monochromator thus had only a small effect on the final result.

For the grazing incidence monochromator a different approach was necessary. Because the lowest energy available from the machine was 40eV no threshold for single ionization was available. The thresholds for the production of doubly, triply, and, in some cases, quadruply charged ions were accessible however and, by tuning the magnetic mass spectrometer to the appropriate position, the variation of the production of the multiply charged ion with respect to the photon energy could be obtained. It was assumed that any signal at energies below the threshold was primarily caused by second order radiation. By comparing this signal with the signal obtained at the appropriate second order wavelengths an estimate of the higher order fraction present was derived. Using this estimate corrections to the ion production rate and the photon signals for both noble gas and molecular oxygen targets were made. The photodiode efficiency was calculated from the noble gas data, and, using this, the relative singly charged molecular oxygen production cross section was determined. A second estimate of the higher order percentage was then made that forced these molecular oxygen cross sections to agree, when normalized, with the previously measured absolute values of Samson et al.[32] This second estimate of the contamination component was then used to recorrect the ion production rates and diode signals. The photodiode efficiency was recalculated and the new

value used to redetermine the molecular oxygen cross section. This procedure was repeated until no further change in the higher order component was necessary. As a check on this higher order subtraction molecular nitrogen was introduced into the collision region and the cross section for the production of molecular nitrogen ions was calculated using the correction factors as determined above. Figure 2 shows both the variation of the molecular oxygen and nitrogen cross sections as a function of wavelength, compared to previously measured data.[32,36] Although the agreement between the present data and the previously measured molecular oxygen cross sections is to be expected the good agreement between the two measurements of the molecular nitrogen cross section acts as a confirmation that the second order subtraction applied to the data is approximately correct.

Oxygen data, taken on both the 4 meter and grazing incidence monochromator, were normalized to the absolute measurements of Samson and Pareek.[21] For the 4 meter data this was done at 584Å since Samson and Pareek had taken considerable care in the laboratory to ensure the accuracy of the cross section measurement at this wavelength. In addition, although the ion signals (taken both with the microwave on and off) revealed considerable structure in the long wavelength region, caused by molecular transitions, the region of 584Å was almost entirely free from them. For the grazing incidence measurements a factor was determined that gave a good fit between the two sets of data over the wavelength range of overlap.

III. RESULTS AND DISCUSSION

The absolute values of the photoionization cross section obtained in the present work are tabulated in Table I for wavelengths between 911 and 260Å. Because multiple ionization cannot occur in this wavelength range the tabulated values represent the total photoionization cross sections. The actual wavelengths used between 911 and 677.5Å, a region of

structure, are tabulated in the first portion of Table I. Towards shorter wavelengths the data have been averaged with the previous results and smoothed to give a best fit to the data. Table II lists the specific cross sections for single, double, and triple photoionization between 254.4 and 44.3Å. The final column of Table II gives the total photoionization cross section.

The present results (not smoothed) are shown in Fig. 3 along with previous experimental results. The present measurements are shown as full circles while the previous data of Samson and Pareek[21] are shown as open circles. Also shown are the experimental results of Kohl et al.[20] (inverted triangles) and those of Comes et al.[19] (triangles). The data at the oxygen K edge, shown at twice the normal scale, were taken from the compilation of Henke et al.[37]

The two points measured by Samson and Pareek[21] at 700.3 and 684.6Å appear to be lower than would be expected. However, examination of the recorder traces reveals that at precisely these wavelengths the ion production rate passes through a minimum because of the influence of the autoionizing resonances leading to the $^2P^\circ$ threshold (see Fig. (5)).

The partial cross sections for producing O^+ in the $^4S^\circ$ ground state and $^2D^\circ$, $^2P^\circ$ excited states are also shown in Fig. 3. These results were obtained from the product of the total atomic cross section and the branching ratios for producing these states. The branching ratios have been measured by the technique of photoelectron spectroscopy at 584Å by Samson and Petrosky[24], at 304Å by Dehmer and Dehmer[25], and between 725 and 580Å by Hussein et al.[26] The dashed lines show a reasonable extrapolation of the present data through the partial cross section points at 584 and 304Å. The full line represents a best fit to the present data, excluding the resonance structure leading to the ^4P threshold. Representative error bars are shown at several points; these were determined from the uncertainty intro-

duced on extracting data from the chart recordings. The overall accuracy of the results depends upon the absolute value of our previous data. An estimated error of ±9% was quoted at that time. However, confidence in the relative and absolute value of the cross sections can be obtained by considering the value of the total oscillator strength for the absorption process. According to the TRK-sum rule[38] the oscillator strength must add up to a value of 8, the total number of electrons in the atom. Thus, we have evaluated the continuum oscillator strength from the ionization threshold down to 44.3Å using the present total photoionization cross sections and from 44.3Å to 0Å using the cross sections from the compilation by Henke et al.[37] A value of 7.29 was obtained. Adding this value to our previously quoted line oscillator strength of 0.71 gives a total oscillator strength of 8.00! Obtaining the precise value of the total oscillator is, of course, fortuitous because the maximum error in the value of the line oscillator strength (±50%) introduces an error of about ±4.4% in the total oscillator strength. However, this implies that our value of the continuum oscillator strength should be accurate to within ±4.4%, which is certainly in keeping with our estimated value of ±9%. It should be noted that in our previous work[21] we did not take into account the effect of multiple ionization below 250Å.

The structure shown in Fig. 3 has not been seen before in photoionization experiments and represents the Rydberg triplet series $2s2p^4(^4P)$ $np(^3D^\circ, {}^3S^\circ, {}^3P^\circ)$. Figure 4 is a trace of the rate meter signal showing the series in detail compared with the theoretical predictions of Pradhan[10]. Also shown are the peak wavelength predictions of Taylor and Burke[8], which agree to within 1Å with those of Pradhan, and the wavelength assignment of Garton and Drew[39] who have observed the series photographically in an absorption experiment and obtained an identification for the $np(^3D^\circ)$ series. As can be seen the agreement between experiment and theory is good, although the shape and position of the third peak of the first

theoretical triplet differs from that measured experimentally; no attempt has been made to allow for peak shifting or broadening of the measured lines caused by the finite resolution of the monochromator.

Figure 5 illustrates the rate meter signal obtained between 760 and 655Å showing the autoionizing resonances leading to the $^2D^\circ$ and $^2P^\circ$ states of the oxygen ion. The wavelengths marked agree to within 0.6Å of the assignments given by Huffmann et al.[22] By comparing the height of the autoionizing peaks with the adjacent continuum a lower limit to the peak cross sections may be determined. For example, the peak to background ratio at 724.8Å is 7.1:1; the adjacent continuum cross section is 8.6 Mb from Fig. 3. Thus, the peak cross section is at least 61 Mb.

Figure 6 shows the high energy measurements of the atomic oxygen photoionization cross section (full circles) compared with those of Samson and Pareek[21] (open circles) to which they have been normalized. Representative error bars are shown and a further 12% caused by systematic error is estimated. The good agreement of the two sets of data in terms of the variation of the cross section with energy also tends to confirm that the higher order subtraction procedure previously detailed is correct.

Figures 7(a) and 7(b) compare most of the presently available theoretical results with our present data plus those of Samson and Pareek (full circle data points). The line previously drawn through the experimental points has been omitted as have the ^4P resonances. The individual theoretical data are identified in the Figures by the initials of the authors as given in parentheses in the following description.

In Fig. 7(a) Bates and Seaton[2] (BS) used Hartree-Fock wave functions to calculate the cross section at the spectral head and then deduced the energy dependence from an approximation given by Bates.[1] Dalgarno et al.[3] (DL, DV) also used Hartree-Fock wave functions for both the bound and continuum orbitals in their calculations of transitions from the ground state

to specific states of the ion. Their data are shown in both the length (L) and velocity (V) approximations. Henry (HL, HV) then investigated the coupling between final state channels, including as many channels as was technically feasible at the time of computation. McGuire[40] (M) used a development of his semiempirical central potential method to calculate the photoionization cross section of all the elements from helium to xenon, including that of oxygen, whereas, Kahler[11] (KA) used the scaled Thomas-Fermi method of Stewart and Rotenberg.[39] Ganas[13] (G) used an independent particle model.

In Fig. 7(b) Taylor and Burke[8] (TB) and Pradhan[10] (P) both introduced close coupling expansions for the initial and final states, but they used different numerical techniques for the solutions, Taylor and Burke employing the R-matrix method while Pradhan used the method of reduction to linear equations; they obtained similar results. Saxon, et al.[16] (SA), also using the R-matrix technique, calculated the photoionization cross section of ground state atoms leading to ground state ions as a preliminary to calculations the cross section for excited oxygen atoms. Their results agree closely with the work of both Taylor and Burke, and Pradhan. Thomas and Helliwell[15] (TH) developed an approximate central potential model for the calculation of the cross section. Koppel[12] (KO) used the scaled Thomas-Fermi method of Stewart and Rotenberg[41], as did Kahler (KA) in Fig. 7(a). The results obtained by the two authors differ considerably. Starace et al.[14] (ST) used Herman-Skillman wave functions in their calculation of the cross section.

Most of the theoretical data lie within ±40% of the experimental data. However, it is interesting to note that at the $^4S^\circ$ ionization threshold the more sophisticated close-coupling and R-matrix calculations show a larger disagreement with experiment than many of the other calculations. The theory that most closely describes the variation of the atomic oxygen ion-

ization cross section is that due to Kahler[11] (see Fig. 7(a)). Many of the others accurately predict the variation of the cross section between ionization onset and the $^2P^\circ$ threshold though agreement is generally poor between the $^2D^\circ$ and $^2P^\circ$ onsets. None of the theories accurately predict the shape of the cross section between the $^2P^\circ$ and ^4P thresholds where the experimental results show a more pronounced peak in the cross section. At higher energies all the theoretical calculations tend to converge towards the experimental results.

ACKNOWLEDGMENTS

This material is based upon work supported by the National Science Foundation under Grant No. ATM-8617670, PHY-8803911, and by the National Aeronautics and Space Administration under Grant No. NGR 28-004-021. It is with pleasure that we acknowledge the help of the personnel at the Stoughton Synchrotron Radiation Center, which is supported by NSF Grant No. DMR-8601349.

REFERENCES

1. D.R. Bates, R.A. Buckingham, H.S.W. Massey, and J.J. Unwin, Proc. Roy. Soc. 170, 322 (1939).
2. D.R. Bates and M.J. Seaton, Mon. Not. Roy. Astr. Soc. 109, 698 (1949).
3. A. Dalgarno, R.J.W. Henry and A.L. Stewart, Planet. Space Sci. 12, 235 (1964).
4. R.J.W. Henry, J. Chem. Phys. 44, 4357 (1966).
5. R.J.W. Henry, Planet. Space Sci. 15, 1747 (1967).
6. R.J.W. Henry, Planet. Space Sci. 16, 1503 (1968).
7. R.J.W. Henry, J. Chem. Phys. 48, 3635 (1968).
8. K.T. Taylor and P.G. Burke, J. Phys. B 9, L353 (1976).
9. A.K. Pradhan and H.E. Saraph, J. Phys. B 10, 3365 (1977).
10. A.K. Pradhan, J. Phys. B 11, L729 (1978).
11. H. Kahler, J. Quant., Spectrosc. Radiat. Transfer. 11, 1521 (1971).
12. J.U. Koppel, J. Chem. Phys. 55, 123 (1971).
13. P.S. Ganas, Phys. Rev. A 7, 928 (1973).
14. A.F. Starace, S.T. Manson, and D.J. Kennedy, Phys. Rev. A 9, 2453 (1974).
15. G.M. Thomas and T.M. Helliwell, J. Quant. Spectrosc. Radiat. Transfer. 10, 423 (1970).
16. R.P. Saxon, R.K. Nesbet, and C.L. Noble, private communication.
17. M.J. Seaton, in "Modern Applications of Atomic and Molecular Processes," ed. A.E. Kingston (Plenum Press, New York, 1988).
18. R.B. Cairns and J.A.R. Samson, Phys. Rev. 139, A1403 (1965).
19. F.J. Comes, F. Speier, and A. Elzer, Z. Naturforsch. 23a, 125 (1968).

20. J.L. Kohl, G.P. Lafyatis, H.P. Palenius, and W.H. Parkinson, Phys. Rev. A 18, 571 (1978).

21. J.A.R. Samson and P.N. Pareek, Phys. Rev. A 31, 1470 (1985).

22. R.E. Huffman, J.C. Larrabee, and Y. Tanaka, J. Chem. Phys. 46, 2213 (1967).

23. P.M. Dehmer, J. Berkowitz, and W.A. Chupka, J. Chem. Phys. 59, 5777 (1973).

24. J.A.R. Samson and V.E. Petrosky, Phys. Rev. A 9, 2449 (1974).

25. J.L. Dehmer and P.M. Dehmer, J. Chem. Phys. 67, 1782 (1977).

26. M.I.A. Hussein, D.M.P. Holland, K. Codling, P.R. Woodruff, and E. Ishiguro, J. Phys. B 18, 2827 (1985).

27. J.A.R. Samson and W.H. Hancock, Phys. Lett. 61A, 380 (1977).

28. G.V. Marr and J.B. West, At. Data Nuc. Data Tables 18, 497 (1976).

29. J.A.R. Samson, in "Advances in Atomic and Molecular Physics" (Academic Press, New York, 1966) Vol. 2, p. 177 and unpublished data.

30. J.A.R. Samson and G.N. Haddad, J. Opt. Soc. Am. 64, 1346 (1974), and G.C. Angel and J.A.R. Samson, unpublished data.

31. P.M. Dehmer and W.A. Chupka, J. Chem. Phys. 62, 4525 (1975).

32. J.A.R. Samson, G.H. Rayborn, and P.N. Pareek, J. Chem. Phys. 76, 393 (1982).

33. N. Jonathan, D.J. Smith, and K.J. Ross, J. Chem. Phys. 53, 3758 (1970).

34. A. Roche, K. Kirby, S.L. Guberman, and A. Dalgarno, J. Electron Spectrosc. Relat. Phenom. 22, 223 (1981).

35. J.A.R. Samson and G.C. Angel, Phys. Rev. (to be published).

36. J.A.R. Samson, T. Masuoka, P.N. Pareek, and G.C. Angel, J. Chem. Phys. 86, 6128 (1987).

37. B.L. Henke, P. Lee, T.J. Tanaka, R.L. Shimabukuro, and B.K. Fujikawa, At. Data. Nuc. Data. Tables 27, 1 (1982).

38. J. Berkowitz, Photoabsorption, Photoionization, and Photoelectron Spectroscopy, (Academic Press, New York, 1979), p. 63.

39. R. Garton and M.D. Drew, private communication, (1976).

40. E.J. McGuire, Phys. Rev. 175, 20 (1968).

41. J.C. Stewart and M. Rotenberg, Phys. Rev. 140, A1508 (1965).

TABLE I. Absolute photoionization cross sections of atomic oxygen between 911 and 260Å. Units are in megabarns (1 Mb = $10^{-18}cm^2$)

λ (Å)	Cross Section (Mb)	λ (Å)	Cross Section (Mb)	λ (Å)	Cross Section (Mb)	λ (Å)	Cross Section (Mb)
911.00	0.15	760.0	3.90	690.6	9.47	490	12.0
910.50	0.70	752.3	4.15	690.0	9.80	structure	
910.00	1.15	732.2	8.03	683.9	9.25	430	11.5
909.80	2.45	730.6	8.40	683.0	9.65	420	11.3
907.50	2.75	729.0	9.17	682.8	9.69	410	11.0
905.00	2.75	727.5	8.90	677.5	10.0	400	11.8
900.00	2.85	722.5	9.02	665.3	12.0	390	10.5
895.00	2.75	720.9	8.91	660	12.6	380	10.2
890.00	2.70	720.0	9.00	650	13.0	370	9.90
885.00	2.85	719.2	9.00	640	13.3	360	9.57
870.00	3.10	717.6	8.79	630	13.4	350	9.25
865.00	3.10	715.7	9.24	620	13.4	340	8.92
860.00	3.10	714.1	9.18	610	13.4	330	8.60
855.00	3.10	712.5	9.26	600	13.3	320	8.25
850.00	3.20	710.8	9.30	590	13.2	310	7.90
845.00	3.25	710.0	9.15	580	13.0	304	7.70*

*Absolute value used for normalization (from ref. 21).

TABLE I. Continued.

λ (Å)	Cross Section (Mb)	λ (Å)	Cross Section (Mb)	λ (Å)	Cross Section (Mb)	λ (Å)	Cross Section (Mb)
840.00	3.30	709.2	9.71	570	12.9	300	7.55
835.00	3.30	707.6	9.88	560	12.7	290	7.40
830.00	3.30	705.9	9.71	550	12.5	280	6.85
825.00	3.30	705.0	9.60	540	12.3	270	6.50
785.00	3.70	695.3	9.06	530	12.1	260	6.15
780.00	3.70	693.8	9.00	520	12.0		
765.00	4.00	692.5	9.60	510	11.9		
760.2	4.06	692.2	9.51	500	11.9		

TABLE II. Absolute photoionization cross section for single, double, and triple photoionization from 44 to 254Å

hν(eV)	λ(Å)	O^+ (Mb)	O^{++} (10^{-2}Mb)	O^{+++} (10^{-3}Mb)	σ_{total} (Mb)
48.736	254.402	6.00	0.0	---	6.00
50	248.0	5.75	2.0	---	5.77
60	206.6	4.25	18.7	---	4.44
70	177.1	3.20	22.5	---	3.43
80	155.0	2.37	23.0	---	2.60
90	137.8	1.84	22.1	---	2.06
100	124.0	1.44	20.5	---	1.65
110	112.7	1.20	18.5	0.28	1.39
120	103.3	1.01	16.4	1.01	1.17
130	95.4	0.86	14.2	1.65	1.00
140	88.6	0.72	12.1	2.02	0.84
150	82.7	0.62	10.3	2.20	0.73
160	77.5	0.52	8.4	2.12	0.61
170	72.9	0.45	6.9	1.95	0.52
180	68.9	0.39	5.8	1.75	0.45
190	65.3	0.33	4.8	1.51	0.38
200	62.0	0.286	3.9	1.28	0.33
210	59.0	0.250	3.2	1.07	0.28
220	56.4	0.220	2.55	0.87	0.25
230	53.9	0.197	2.05	0.69	0.22
240	51.7	0.180	1.75	0.54	0.20
250	49.6	0.168	1.50	0.44	0.18
260	47.7	0.161	1.30	0.37	0.17
270	45.9	0.154	1.20	0.32	0.17
280	44.3	0.150	1.05	0.27	0.16

Figure Captions

1. Schematic diagram of the apparatus showing the side view (upper diagram) and end view (lower diagram) as seen from M looking towards D (for symbols see text).
2. The photoionization cross section for production of O_2^+ from O_2 (left ordinate) and N_2^+ from N_2 (right ordinate). O, present data; O, (O_2^+), Samson et al. (ref. 32); Δ, (N_2^+), Samson et. al. (ref. 36).
3. The photoionization cross section of atomic oxygen for the production of singly charged ions as a function of wavelength. O, present data; O, previous data, Samson and Pareek (ref. 21); ∇, Kohl et al. (ref. 20); Δ, Comes et al. (ref. 19). Partial cross sections; , Hussein et al. (ref. 26); , Dehmer and Dehmer (ref. 25); solid circles with error bars at 584Å, Samson and Petrosky (ref 24).
4. The autoionizing resonances leading to the ^4P threshold; upper curve, the rate meter signal from the present experiment; lower curve, the theoretical predictions of Pradhan (ref. 10). The upper wavelength assignments are those derived from the present work and the photographic measurements of Garton and Drew (ref. 39), the lower are those reported by Pradhan (ref. 10), and Taylor and Burke (ref. 8).
5. The ratemeter signal in the present experiment showing the autoionizing resonances leading to the $^2D^\circ$ and $^2P^\circ$ ion thresholds. The wavelength assignments are derived from the present work. The dashed line represents the decrease in the stored ring current over the period that the scan was made and is thus proportional to the photon flux.
6. The high energy region of the photoionization cross section of atomic oxygen leading to the production of singly charged ions. O, present data; O, previous data of Samson and Pareek (ref. 21).

7. A comparison of the experimental and theoretical photoionization cross sections of atomic oxygen. In both 7(a) and 7(b) the full circles represent the combined data of the present experiment and the previous measurements of Samson and Pareek (ref. 21). Theoretical estimates:

7(a):

BS, Bates and Seaton, ref. 2

DL, – – – – Dalgarno et al. (length formulation), ref. 3

DV, -x-x Dalgarno et al. (velocity formulation)

HL, –·–· Henry (length formulation), refs. 5 and 6

HV, –··–·· Henry (velocity formulation)

M, ∇∇∇ McGuire, ref. 40

G, -xx-xx Ganas, ref. 13

KA, 000 Kahler, ref. 11

7(b):

TB, – – – Taylor and Burke (length formulation), ref. 8

P, -x-x Pradhan, ref. 10

TH, –··–·· Thomas and Helliwell, ref. 15

KO, –·–· Koppel, ref. 12

ST, Starace et al., ref. 14

SA, -xx-xx Saxon et al., ref. 16

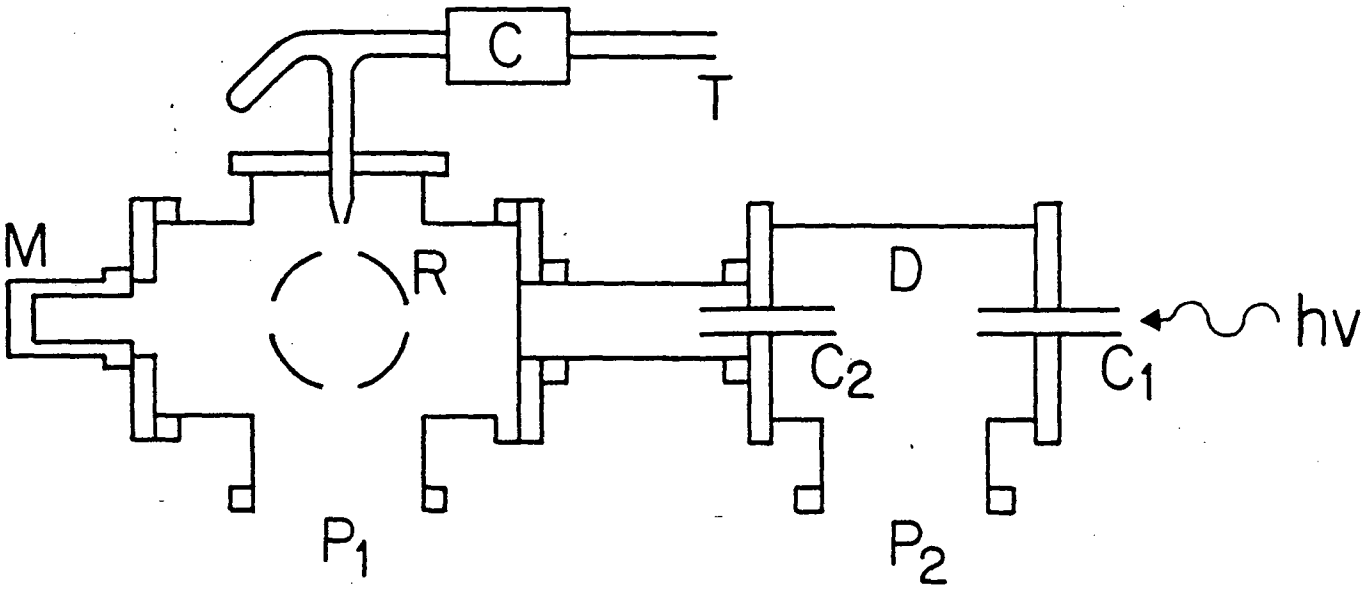
C
T
M
R
D
hv
C2
C1
P1
P2

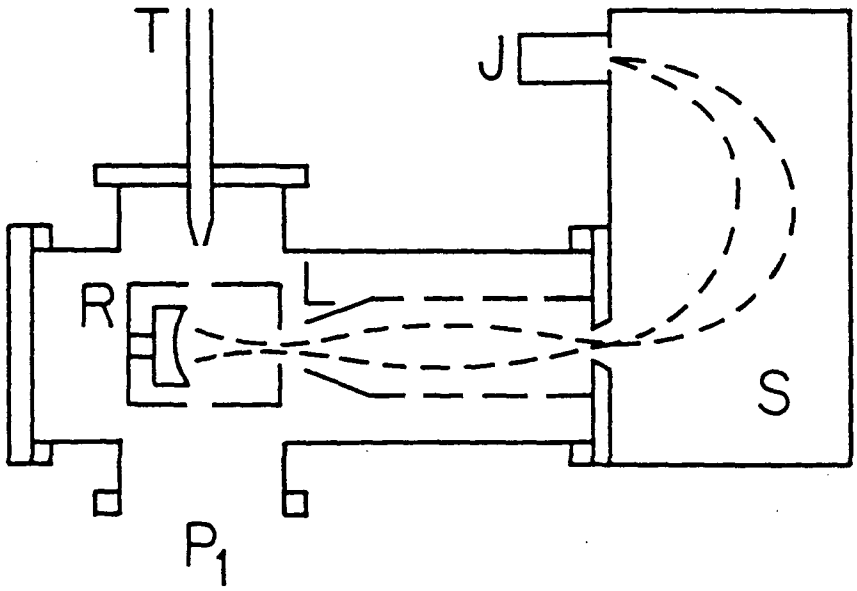
T
J
R
S
P1

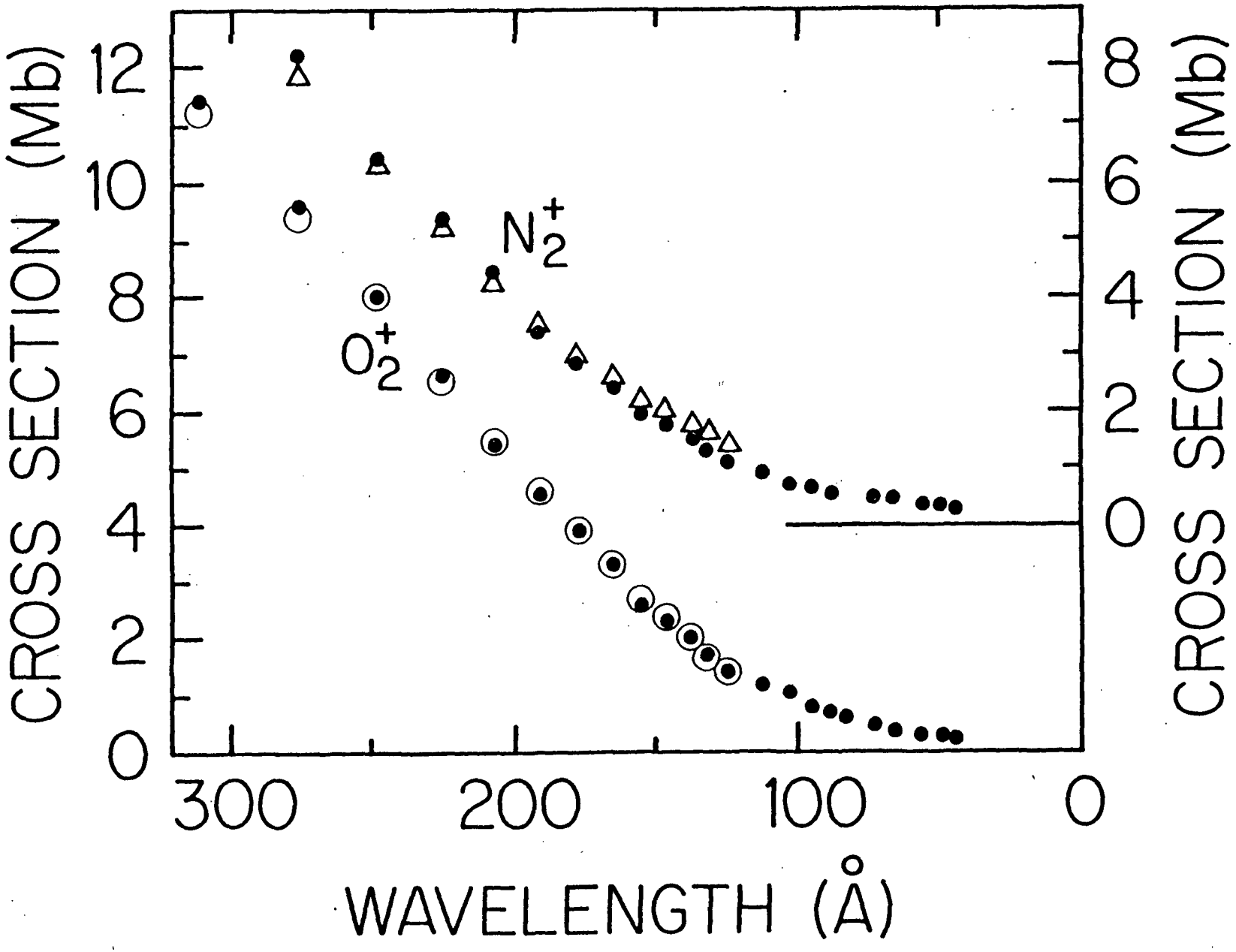
CROSS SECTION (Mb)
12
10
8
6
4
2
0
N_2^+
O_2^+
300
200
100
0
WAVELENGTH (Å)
8
6
4
2
0
CROSS SECTION (Mb)

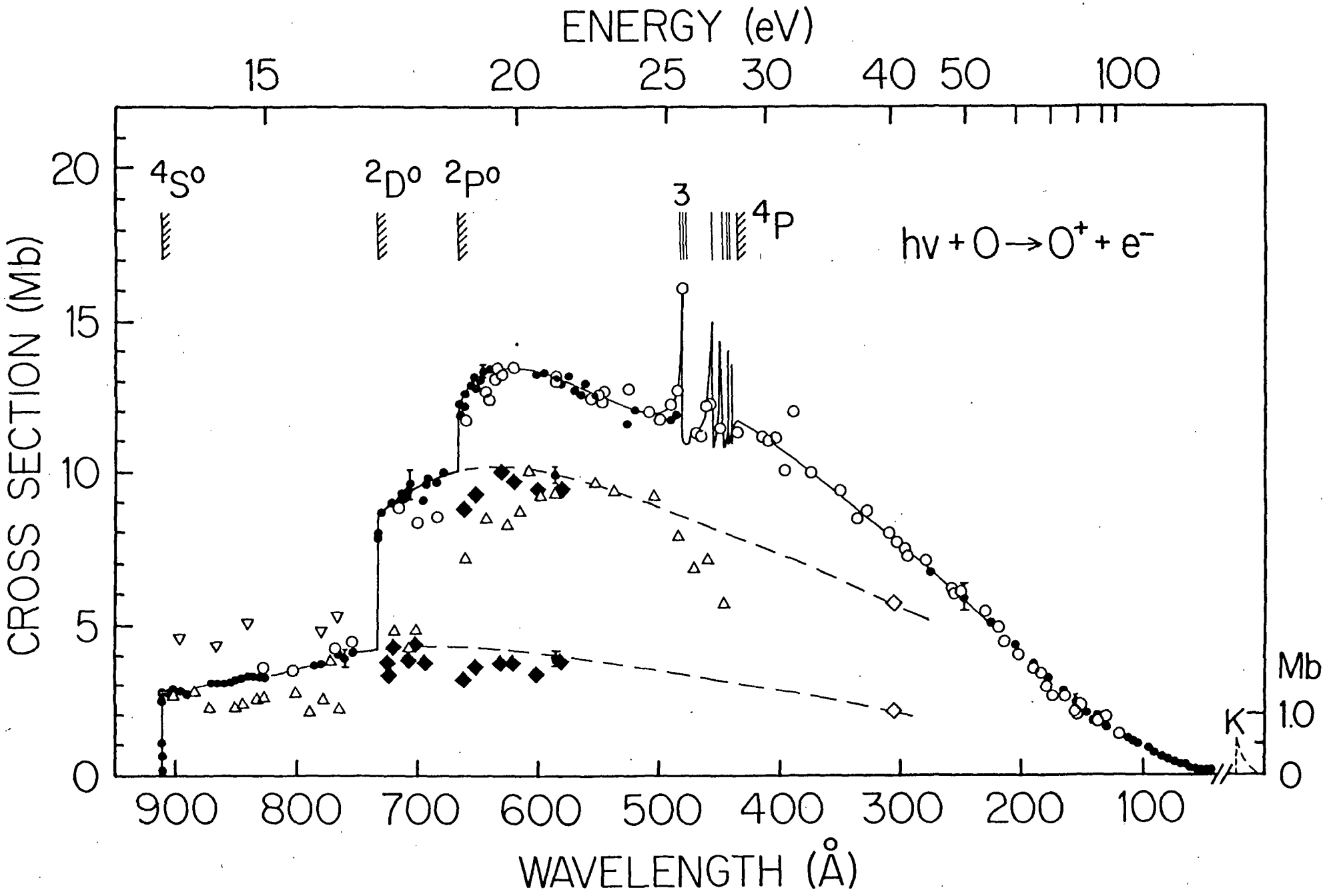
ENERGY (eV)
15
20
25
30
40
50
100
$^4S^o$
$^2D^o$
$^2P^o$
3
^4P
$h\nu + O \rightarrow O^+ + e^-$
CROSS SECTION (Mb)
20
15
10
5
0
Mb
1.0
0
K
900
800
700
600
500
400
300
200
100
WAVELENGTH (Å)

OI $2s2p^4(^4P)np(^3D^o, ^3S^o, ^3P^o)$ SERIES

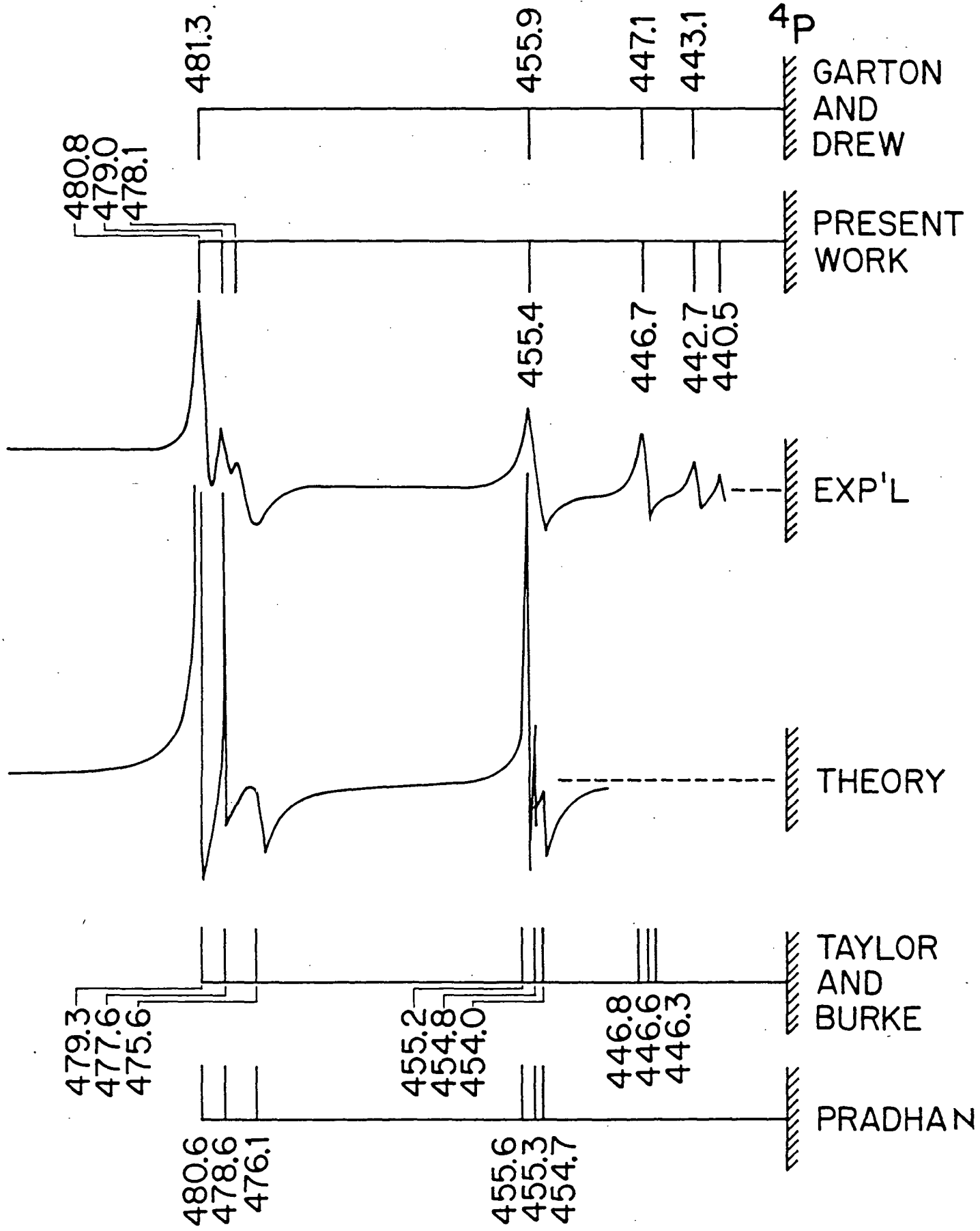

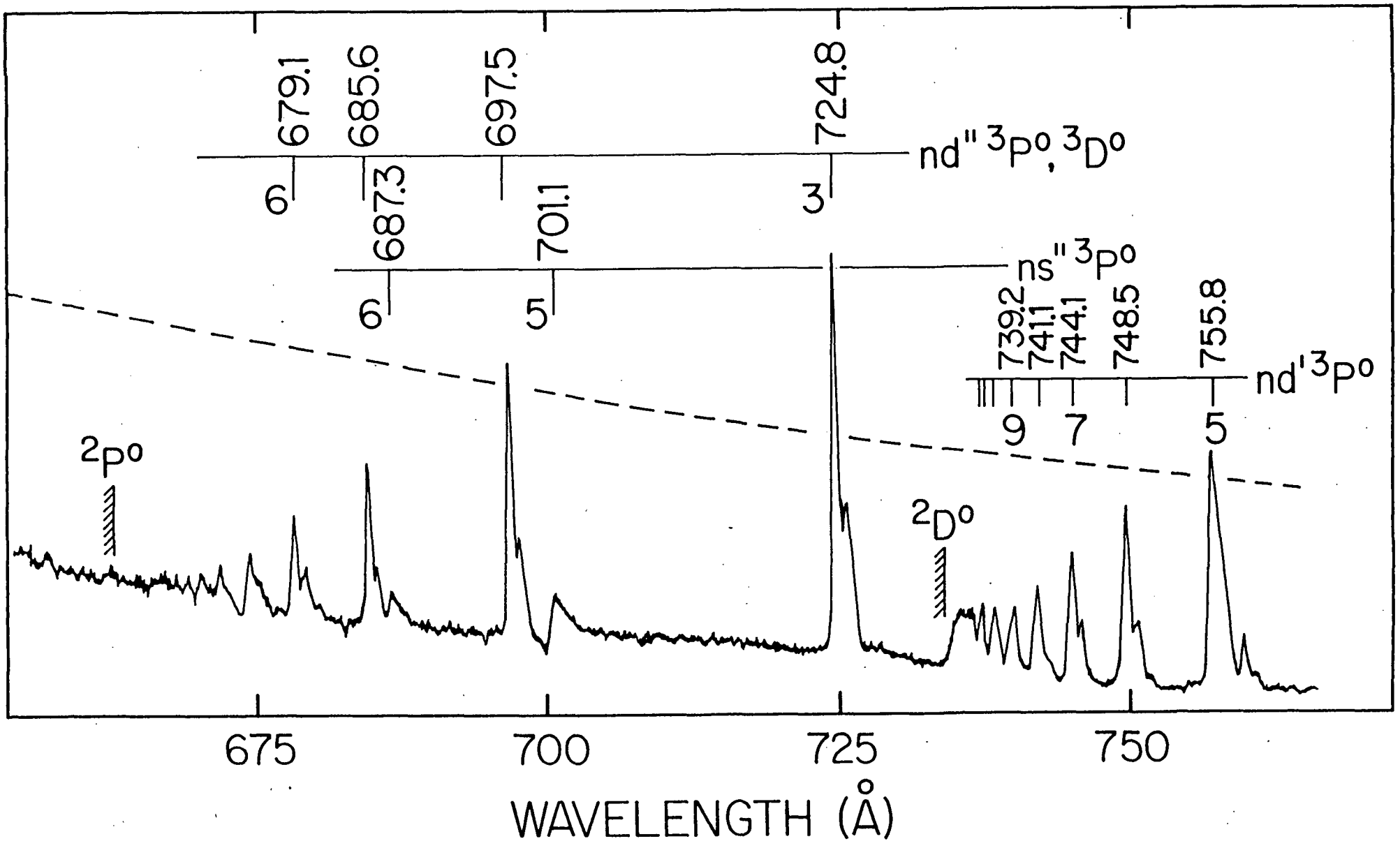
679.1
685.6
697.5
724.8
nd'' 3P°, 3D°
6
6873
701.1
3
ns'' 3P°
6
5
739.2
741.1
744.1
748.5
755.8
nd' 3P°
9
7
5
2P°
2D°
675
700
725
750
WAVELENGTH (Å)

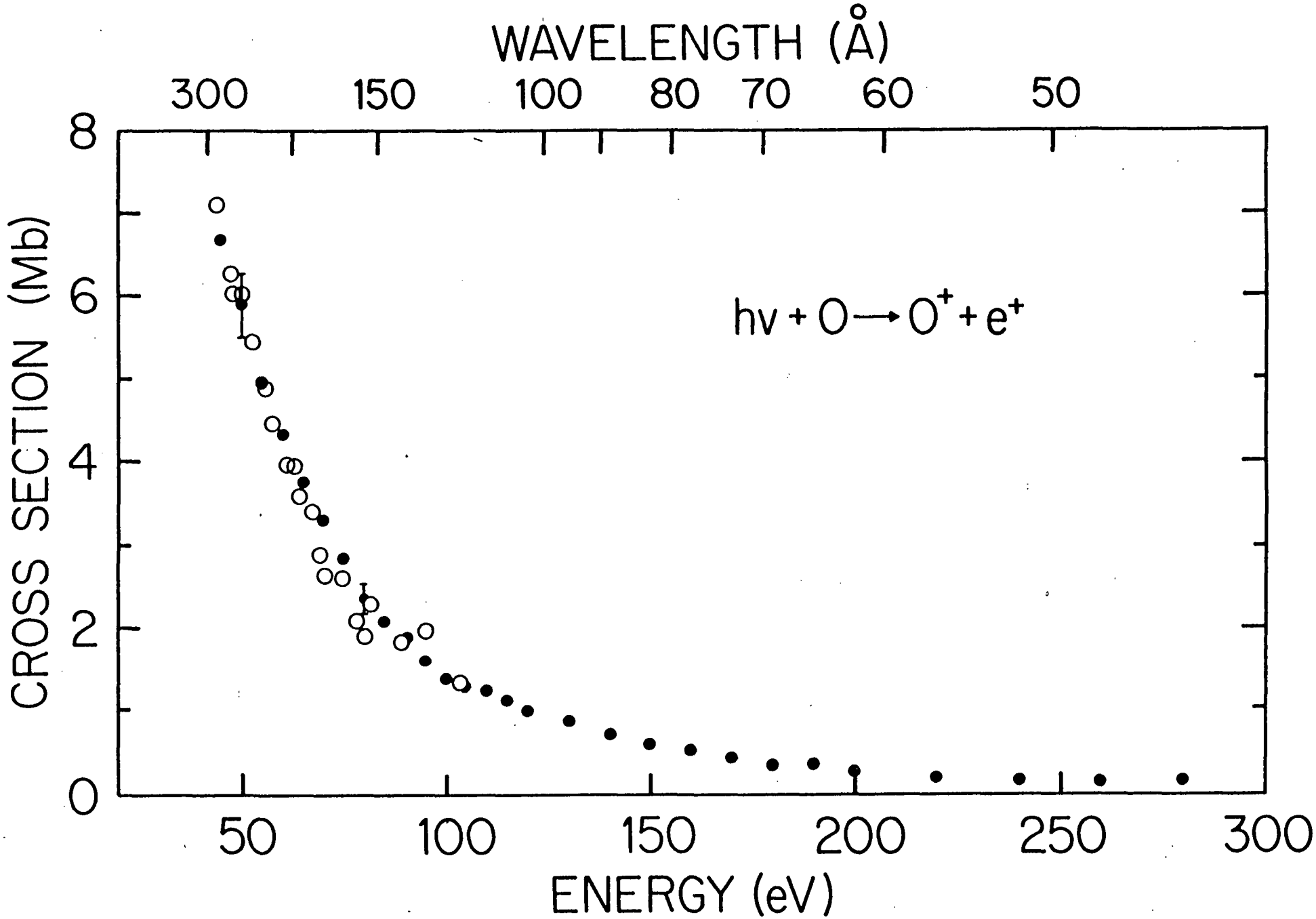
WAVELENGTH (Å)
300
150
100
80
70
60
50
CROSS SECTION (Mb)
0
2
4
6
8
hν + O → O+ + e+
50
100
150
200
250
300
ENERGY (eV)

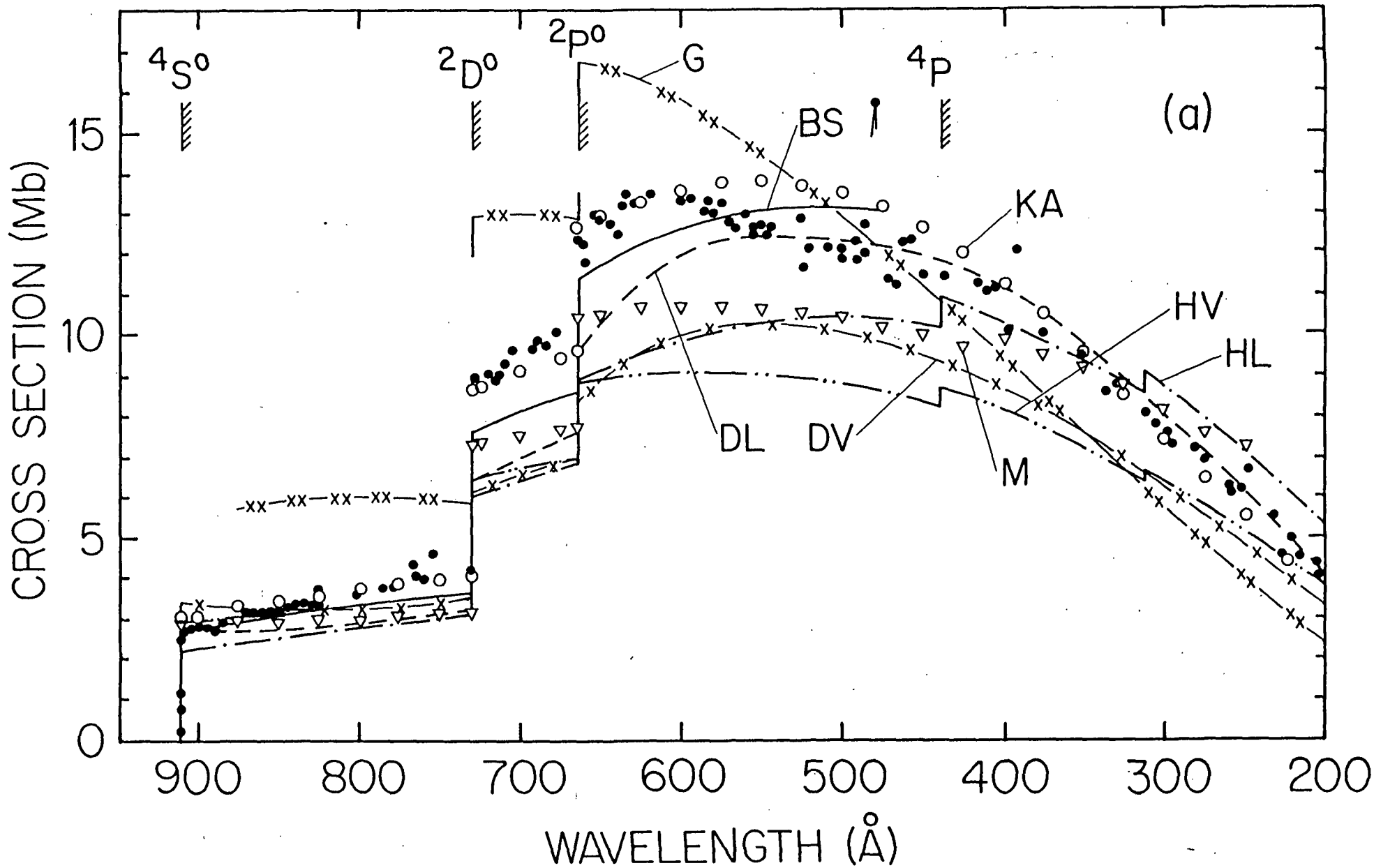
4S°
2D°
2P°
G
BS
4P
(a)
KA
HV
HL
DL
DV
M
CROSS SECTION (Mb)
0
5
10
15
900
800
700
600
500
400
300
200
WAVELENGTH (Å)

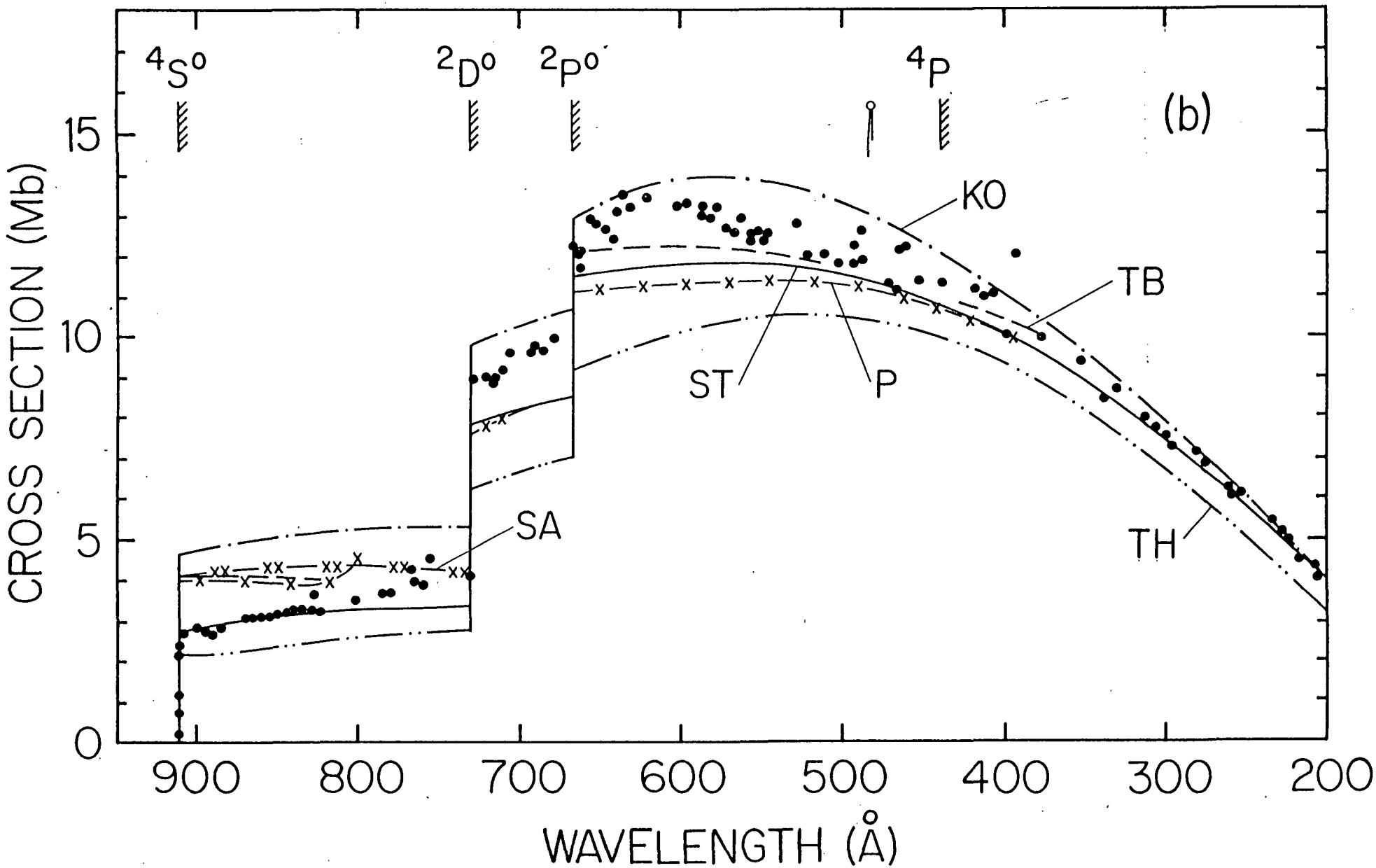
$^4S^o$
$^2D^o$
$^2P^o$
^4P
(b)
KO
TB
ST
P
SA
TH
CROSS SECTION (Mb)
0
5
10
15
900
800
700
600
500
400
300
200
WAVELENGTH (Å)